Prabha Materials Science Letters
Vol. 4, No. 1, 57-65, 2025
https://doi.org/10.33889/PMSL.2025.4.1.005

Ram Arti Publishers

Enhanced Short Wavelength Infrared Absorption in Tri-Layer Metamaterials through Polymer Coating

Harshita Chawla
Department of Physics,
Teerthanker Mahaveer University Moradabad, Moradabad, 244001, Uttar Pradesh, India.
E-mail: harshitar0704@gmail.com

Vishnu Prasad Shrivastava
Department of Physics,
Teerthanker Mahaveer University Moradabad, Moradabad, 244001, Uttar Pradesh, India.
Corresponding author: vishnu.shrivastava.indus@gmail.com

(Received on September 29, 2024; Revised on November 9, 2024; Accepted on November 10, 2024)

Abstract
A highly efficient absorption in the short wavelength infrared (SWIR) spectral region is essential for the advancement of technologies in energy harvesting, infrared detection, and thermal emission. This study presents a polymer-coated multilayer perfect absorber metamaterial (MPA) with enhanced performance in the SWIR range. The MPA structure comprises four layers: a Polymethyl Methacrylate (PMMA) polymer top layer, an array of circular Titanium Nitride (TiN) disks as the second layer, thin film of Zinc Oxide (ZnO) as the dielectric middle layer, and a thin Titanium Nitride (TiN) film as the bottom metallic layer. Our findings demonstrate that this MPA achieves near-perfect absorption of 99% at a wavelength of 1.3 µm. The absorption characteristics are further investigated with respect to various structural parameters to ensure better performance of the absorber. The absorber holds great potential for applications in energy absorption, infrared sensing, thermal emission, and related fields.

Keywords- Perfect absorber, Metamaterials, SWIR, LSPR resonance, Titanium nitride (TiN), Optical materials.

1. Introduction

Metamaterials are artificially engineered materials designed to possess unconventional properties not found in natural substances, such as negative perfect absorption (Landy et al., 2008; Shrivastava et al., 2023; Wang et al., 2024a), epsilon zero effect (Pianelli et al., 2024; Rensberg et al., 2017), refractive index (Kaina et al., 2015; Khouser and Choukiker, 2024), modification of emission (Kumar et al., 2018; Kumar and Mitra, 2023; Shrivastava et al., 2018) etc. Metamaterials with near-total absorption within specific electromagnetic spectral regions, known as metamaterial perfect absorbers (MPAs), have wide applications in stealth technology (Abdulkarim et al., 2020), thermal emission (Landy et al., 2008), solar cells (Jeon et al., 2015; Wu et al., 2023), bolometers (Dao et al., 2019), and sensing (Ren et al., 2020; Shakiba et al., 2024; Xiong et al., 2022). Metamaterials are generally structured as three layers—metal, dielectric and metal. The top layer is made with the periodic pattern of metallic structure (resonant layer), and middle (spacer layer) and bottom layer are formed by the plane thin film of dielectric and metal materials respectively (Chai et al., 2022; Farooq et al., 2022; Rhee et al., 2014). Perfect absorption in these structures arises when incident electromagnetic waves interact with the resonant metallic structure, creating opposing currents in both the upper and bottom metal films, which induces magnetic field in the spacer layer. By optimizing both electric and magnetic resonances, MPAs can achieve impedance matching with the surrounding environment, leading to reduced reflectance and enhanced absorption(Wang et al., 2024b).

Noble Metals (i.e. gold, silver, aluminium, and copper) are excellent in light absorption due to their unique optical properties make them useful in high-performance metamaterial absorber development. Their strong resonances, driven by surface plasmon resonances (SPRs), enhance absorption efficiency by collectively oscillating free electrons in response to incident electromagnetic waves. These metals boast the highest light absorption efficiency across visible, near-infrared (NIR), and short-infrared spectrums(Dubey et al., 2022; Jaiswal et al., 2023; Watts et al., 2012; Yu et al., 2023). However, they are expensive, ohmic losses contributing to heat generation, limited tunability, challenges in nanostructure fabrication, and compatibility issues limit their multiple use (Chen et al., 2016; Sun et al., 2018). Thus, there's a demand for alternative plasmonic materials for replacing noble metal to lower costs and to reduce ohmic losses. New plasmonic materials like doped oxides and nitrides, such as transparent conducting oxides and transition metal nitrides, offer reduced material loss and hold promise for constructing low-loss plasmonic and metamaterial structures with sharper resonances and higher field concentrations. Due to its high corrosion and temperature resistance, as well as mechanical strength and durability (Liu et al., 2018), TiN has grown interest as a plasmonic layer in metamaterials. For instance, Liu et al. uses tin nitride (TiN) based structure to obtain a perfect solar absorber (Liu et al., 2018). However, TiN did not used as plasmonic layer for absorbing SWIR spectral region.

In this paper, we propose a novel design for a four-layer multilayered Metamaterial Perfect Absorber (MPA) aimed at achieving near-unity absorption centered on the 1.3 µm SWIR spectral region. The structure consists of a top layer of polymethyl methacrylate (PMMA) coating an array of titanium nitride (TiN) disks, followed by a Zinc Oxide (ZnO) dielectric spacer in the middle, and a thin-film TiN layer at the base. This arrangement—PMMA/TiN/ZnO/TiN—defines the multilayer composition of the MPA.

Zinc Oxide (ZnO) was selected as the spacer layer due to its beneficial properties: a high dielectric constant (~2.1) that enables strong electric field confinement to support resonances for near-unity absorption, broad optical transparency to minimize unwanted absorption, and compatibility with plasmonic materials like Titanium Nitride (TiN), enhancing structural stability and thermal resilience. These attributes make ZnO an ideal choice for achieving targeted SWIR absorption in the MPA design. The PMMA polymer coating, serving as the topmost layer, further enhances the absorber's performance by providing optimal environmental stability, protecting the TiN disks, and allowing fine-tuning of resonances through its refractive properties, which improve coupling with incident SWIR light. To our knowledge, no studies have yet shown sharp absorption in the SWIR region using this particular structural design which makes it potential research for applications in plasmonic sensor (Liu et al., 2010; Shrivastava et al., 2017), thermal cooler/emitter (Chen et al., 2016; Hossain et al., 2015), stealth coatings that can conceal objects from infrared detectors and night-vision devices (Kim et al., 2017; Şanlı et al., 2024) etc.

2. Designing and Simulation

Figure 1(a) presents a cross-sectional view of the unit cell structure for the optimized metamaterial perfect absorber (MPA) along the x-y plane, while **Figure 1(b)** provides the top view along the z-y plane. As described earlier, the MPA is composed of four distinct layers. The top polymer layer is of Polymethyl methacrylate (PMMA) followed by a two-dimensional Titanium Nitride (TiN) disk array and a bottom conducting layer of TiN which is separated by a ZnO dielectric spacer layer. The MPA hereafter is denoted by PMMA/TiN/ZnO/TiN. In **Figure 1(a)**, the parameter ‘s’, ‘t’, ‘h’, and ‘g’ represent the thicknesses of the PMMA film, TiN disk, ZnO dielectric middle flim, and TiN ground layer, respectively. The disc radius is represented by ‘r′ and the period of the unit cell is denoted by ‘p′ respectively, as shown in **Figure 1(a)**. The optimized structural values are: p = 300 nm, r = 110 nm, t = 25 nm, s = 40 nm, h = 50 nm, and g = 100 nm.

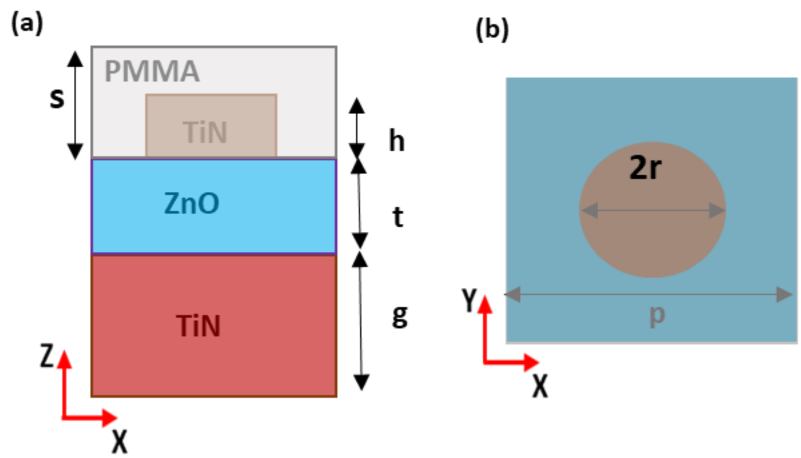

Figure 1. Schematic diagram of the unit cell for the PMMA/TiN/ZnO/TiN Metamaterial Perfect Absorber (MPA) structure, showing (a) a cross-sectional view along the z-x plane and (b) a top view along the y-x planes. Here, 's', 't', 'h', and 'g' represent the thicknesses of the PMMA film, TiN disk, ZnO spacer layer, and TiN bottom layer, respectively. The parameters 'r' and 'p' denote the disk radius and the periodicity of the unit cell.

A numerical simulation was carried out on the unit cell of the MPA using the finite-difference time-domain (FDTD) method within COMSOL Multiphysics software to evaluate its resonant characteristics. A normally incident electromagnetic wave, directed along the z-axis, was used to illuminate the top xy-plane of the structure. Unit cells were configured in the xy-plane to create an infinite array, with boundary conditions applied accordingly. The dielectric permittivity for TiN, represented as 'ε(ω)', was determined using the Drude-Lorentz dispersion model.

$$\varepsilon(\omega) = \varepsilon_\infty + \frac{f_0 \omega_p{}^2}{\omega_0{}^2 - \omega^2 + i\Gamma_0 \omega} \quad (1)$$

In this model ε_∞, f_0, ω_p, ω_0 and Γ_0 represents background permittivity, oscillator strength, plasma frequency, resonant frequency and damping frequency, respectively. The parameter values applied for TiN are as follows: ω_p=1.2049e16 rad/sec, Γ_0= 2.2271e14 rad/sec, ε_∞ = 4.855 as given in reference(Naik et al., 2013). The values of dielectric constant of PMMA and ZnO are obtained from the reference (Zhang et al., 2020) and (Hakim et al., 2022) respectively. The absorption is further calculated from the following equation:

$$A(\omega) = 1 - R(\omega) - T(\omega) \quad (2)$$

where, R (ω) and T (ω) represents the coefficient of reflection and transmission, respectively. The Equation (2) can also be written as in terms of S-parameters:

$$A(\omega) = 1 - |S_{11}(\omega)|^2 - |S_{21}(\omega)|^2 \quad (3)$$

where, $S_{11}(\omega)$ represents the reflection coefficients and $S_{21}(\omega)$ denotes the transmission coefficient, respectively. The transmittance can be taken as zero due to presence of TiN in the proposed metamaterial (i.e. $S_{21}(\omega)$ or $T(\omega) = 0$). Therefore, the absorption depends due to $S_{11}(\omega)$ only. The Equation (3) can be reduced to

$$A(\omega) = 1 - |S_{11}(\omega)|^2 \quad (4)$$

Thus, the absorption of the electromagnetic waves in the metamaterial absorber can be modify by tuning its impedance.

3. Results and Discussion

Figure 2 (**a** and **b**) show the simulated optical properties of the PMMA coated MPA (i.e. PMMA/TiN/ZnO/TiN) and without PMMA coated MPA (i.e TiN/ZnO/TiN) structure in infra- red regions. **Figure 2(a)** depicts the absorptance (A), transmittance (T), and reflectance (R) spectra of PMMA/TiN/ZnO/TiN MPA in the range of 0.8- 2 µm. It displays a distinct sharp absorption band in the range of ~ 1 - 1.8 µm covering most of the spectral range of SWIR region. It can be seen that the absorption peak appeared at 1.3 µm (say Mode-A) with the absorptance intensity of > 99% and width ~ 0.15 µm. **Figure 2(b)** depicts the absorptance (A), transmittance (T), and reflectance (R) spectra of TiN/ZnO/TiN MPA in the range of 0.8- 2 µm. It can be seen that the absorption peak appeared at 1.35 µm with absorption intensity upto 80 % and have the peak width of 0.24 µm. This suggests that the polymer coated MPA possesses nearly perfect absorption (> 99%) in SWIR spectral region in contrast to without polymer coated MPA (~ 80%). Also, the coated MPA have sharper absorption peak which make more suitable for sensing applications.

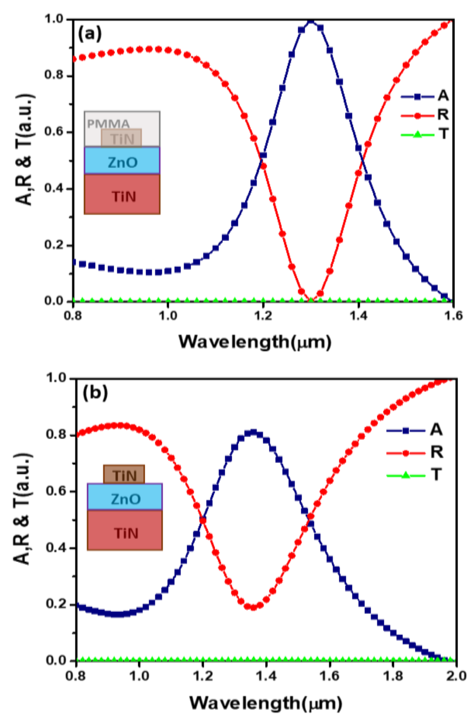

Figure 2. Simulated absorbance spectrum of (a) PMMA/TiN/ZnO/TiN MPA and (b) TiN/ZnO/TiN MPA structure for SWIR wavelength range. Parameters: thickness of spacer layer h= 50 nm disk thickness t= 25 nm, thickness of bottom layer g= 100 nm, disk radius r = 110 nm, and period p = 300 nm.

To understand the mechanism of the resonance absorption in the PMMA/TiN/ZnO/TiN MPA, the electric and magnetic field intensity distributions along the X-Z plane are shown in **Figure 3** (**a** and **b**). These results clearly illustrate (i) the dipolar behavior of the electric field at the corners of the TiN disk (**Figure 3(a)**) and, (ii) the magnetic field at the middle of the ZnO spacer (**Figure 3(b)**), which are the characteristic of fundamental dipole arising at 1.3 µm. Therefore, when the SWIR electromagnetic radiation impinges on this structure, it excites the electric dipoles at the corners of the TiN disks due to their high conductivity and plasmonic properties. This results in surface current fluxes at both the top TiN disk and the bottom TiN layer, flowing in opposite directions. These anti-parallel currents create a circulating current that induces a strong magnetic field within the ZnO spacer, supporting simultaneous electric and magnetic resonances. These resonances are essential for achieving impedance matching with free space, minimizing reflection, and maximizing absorption of the incident waves. Additionally, the optimized thicknesses of the PMMA, ZnO, and TiN layers ensure constructive and destructive interference effects that further enhance absorption. Pradhan et al. (2020) also observed such interference effect in the dielectric coated metamaterial (Pradhan et al., 2020). Thus, the combined effect of material properties and geometric design results in the effective trapping and dissipation of electromagnetic energy, leading to near-perfect absorption of the SWIR spectrum by the MPA.

To explore the absorption behavior in more detail, the MPA is analyzed by varying its geometric parameters. **Figure 4 (a-c)** illustrates the absorbance spectra of the PMMA/TiN/ZnO/TiN MPA as a function of the PMMA layer thickness (s), TiN disk radius (r), and thickness of spacer (h). **Figure 4(a)** shows the absorptance spectra of PMMA/TiN/ZnO/TiN MPA by increasing the thickness of PMMA coating from 20 nm to 80 nm. It indicates that the absorptance peak of fundamental mode increases on increasing the coating thickness up to 40 nm and then decreases afterwards. It clear that an increase on coating thickness also leads to a shifting of peak position from 1.22 to 1.34 µm. **Figure 4(b)** show the variation of absorption spectra of MPA with respect to the disk diameter (r). One can see that Mode-A is red-shifted significantly with increasing the disk diameter which is typical nature of fundamental dipole mode. **Figure 4(c)** depicts the absorbance spectra of MPA by increasing the spacer layer thickness from 20 nm to 60 nm. It indicates that the absorbance intensity of fundamental mode increases on increasing the spacer layer thickness with small shift in peak position. This confirms that the origin of the resonance mode arises from the simultaneous excitation of both electric and magnetic fields.

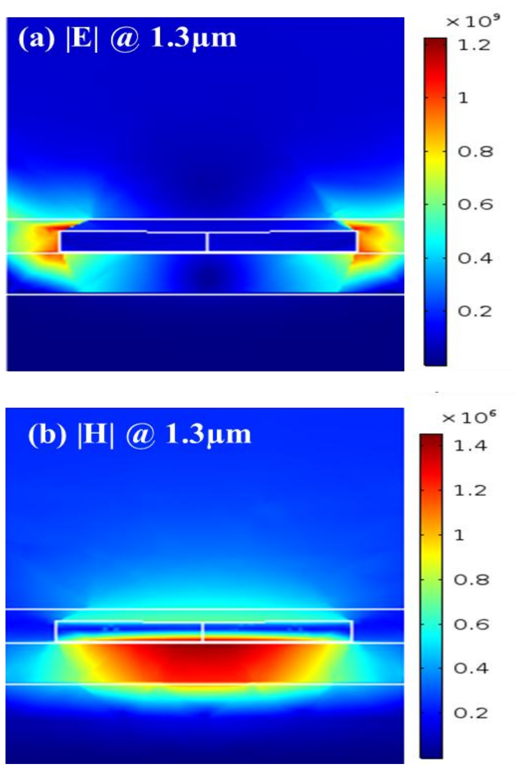

Figure 3. (a) Normalized electric field (|E|) and (b) magnetic field (|H|) distribution of PMMA/TiN/ZnO/TiN MPA along z-x plane.

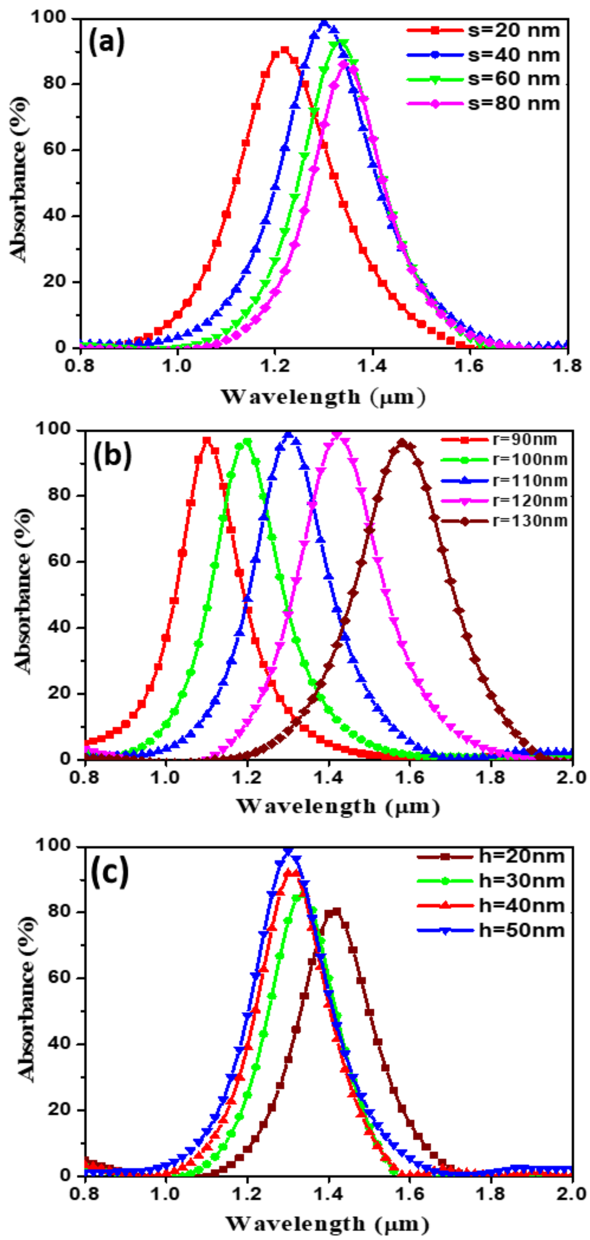

Figure 4. Simulated absorbance spectrum and the corresponding line plot of absorption peak position of PMMA/TiN/ZnO/TiN MPA at various:(a) thickness 's' of PMMA coating, (b) disk radius 'r', (c) spacer layer thickness 'h'.

4. Conclusions

In this study, we have designed a PMMA-coated perfect absorber metamaterial (PMMA/TiN/ZnO/TiN) that achieves efficient absorption in the short-wavelength infrared (SWIR) region, addressing the need for precise spectral control in this range. Using the finite-difference time-domain (FDTD) method, we analyzed the absorption characteristics of this four-layer structure, which includes a periodic TiN disk array on a ZnO dielectric spacer, with a TiN ground layer and a protective PMMA coating on top. Through optimization of key parameters—PMMA coating thickness, disk diameter, spacer layer height, and unit cell size—we achieved near-perfect absorption (>99%) within the 1.25–1.35 μm wavelength range. This study closes the gap in high-absorption SWIR metamaterials by offering an optimized design with significant spectral precision, supported by structural parameters such as a disk radius of 110 nm and thickness of 25 nm, a unit cell size of 400 nm, a ZnO spacer thickness of 50 nm, and a TiN ground layer thickness of 100 nm at normal incidence. This design's robust performance demonstrates the potential of structured metamaterials for applications like plasmonic sensors, thermal emitters, and stealth technology, where controlled SWIR absorption is crucial.

Conflict of Interest

The authors declare that they have no conflict of interest regarding the publication of this article.

Acknowledgments

The authors acknowledge Prof. Jitendra Kumar and the Indian Institute of Technology Kanpur, India, for their valuable support.

References

Abdulkarim, Y. I., Deng, L., Luo, H., Huang, S., He, L., Yuhan, L., Muhammadsharif, F.F., Altintaş, O., Sabah, C., & Karaaslan, M. (2020). Electromagnetic simulations of polarization-insensitive and wide-angle multiband metamaterial absorber by incorporating double asterisk resonator. *Bulletin of Materials Science, 43*(1), 116. https://doi.org/10.1007/s12034-020-02098-3.

Chai, M., Wang, Y., Chen, C., Zhao, Z., Jin, M., & He, T. (2022). Metamaterials-based photoelectric conversion: from microwave to optical range. *Laser & Photonics Reviews, 16*(3), 2100458. https://doi.org/10.1002/lpor.202100458.

Chen, Z., Zhu, L., Raman, A., & Fan, S. (2016). Radiative cooling to deep sub-freezing temperatures through a 24-h day–night cycle. *Nature Communications, 7*(1), 13729. https://doi.org/10.1038/ncomms13729.

Dao, T.D., Doan, A.T., Ngo, D.H., Chen, K., Ishii, S., Tamanai, A., & Nagao, T. (2019). Selective thermal emitters with infrared plasmonic indium tin oxide working in the atmosphere. *Optical Materials Express, 9*(6), 2534-2544.

Dubey, S.K., Kumar, A., Dayal, G., Pathak, A., & Srivastava, S.K. (2022). Polarization insensitive metamaterial based electromagnetic multiband absorber in the long-wave infrared (LWIR) region. *Optics & Laser Technology, 156*, 108511. https://doi.org/10.1016/j.optlastec.2022.108511.

Farooq, S., Rativa, D., Said, Z., & Araujo, R.E.D. (2022). Ultra-sensitive narrow-band plasmonic perfect absorber for sensing applications. *Photonics and Nanostructures - Fundamentals and Applications, 50*, 101018. https://doi.org/10.1016/j.photonics.2022.101018.

Hakim, M.L., Hanif, A., Alam, T., Islam, M.T., Arshad, H., Soliman, M.S., Albadran S.M., & Islam, M.S. (2022). Ultrawideband polarization-independent nanoarchitectonics: a perfect metamaterial absorber for visible and infrared optical window applications. *Nanomaterials*, *12*(16), 2849. https://doi.org/10.3390/nano12162849.

Hossain, M.M., Jia, B., & Gu, M. (2015). A metamaterial emitter for highly efficient radiative cooling. *Advanced Optical Material, 3*(8), 1047-1051.

Jaiswal, A., Rastogi, C.K., Rani, S., Singh, G.P., Saxena, S., & Shukla, S. (2023). Two decades of two-photon lithography: materials science perspective for additive manufacturing of 2D/3D nano-microstructures. *Iscience, 26*(4), 106374. https://doi.org/10.1016/j.isci.2023.106374.

Jeon, N.J., Noh, J.H., Yang, W.S., Kim, Y.C., Ryu, S., Seo, J., & Seok, S.I. (2015). Compositional engineering of perovskite materials for high-performance solar cells. *Nature, 517*(7535), 476-480. https://doi.org/10.1038/nature14133.

Kaina, N., Lemoult, F., Fink, M., & Lerosey, G. (2015). Negative refractive index and acoustic superlens from multiple scattering in single negative metamaterials. *Nature*, *525*(7567), 77-81. https://doi.org/10.1038/nature14678.

Khouser, G.H., & Choukiker, Y.K. (2024). Design of negative refractive index 3D metamaterial split ring resonator for IoT applications. *Microwave and Optical Technology Letters, 66*(1), e33443.

Kim, J., Han, K., & Hahn, J.W. (2017). Selective dual-band metamaterial perfect absorber for infrared stealth technology. *Scientific Reports, 7*(1), 1-9.

Kumar, A., Srivastava, Y.K., Manjappa, M., & Singh, R. (2018). Color-sensitive ultrafast optical modulation and switching of terahertz plasmonic devices. *Advanced Optical Materials, 6*(15), 1800030. https://doi.org/10.1002/adom.201800030.

Landy, N.I., Sajuyigbe, S., Mock, J.J., Smith, D.R., & Padilla, W.J. (2008). Perfect metamaterial absorber. *Physical Review Letters, 100*(20), 207402.

Liu, N., Mesch, M., Weiss, T., Hentschel, M., & Giessen, H. (2010). Infrared perfect absorber and its application as plasmonic sensor. *Nano Letters, 10*(7), 2342-2348. https://doi.org/10.1021/nl9041033.

Liu, Z., Liu, G., Huang, Z., Liu, X., & Fu, G. (2018). Ultra-broadband perfect solar absorber by an ultra-thin refractory titanium nitride meta-surface. *Solar Energy Materials and Solar Cells, 179*, 346-352. https://doi.org/10.1016/j.solmat.2017.12.033.

Naik, G.V., Shalaev, V.M., & Boltasseva, A. (2013). Alternative plasmonic materials: beyond gold and silver. *Advanced Materials, 25*(24), 3264-3294.

Pianelli, A., Dhama, R., Judek, J., Mazur, R., & Caglayan, H. (2024). Si-CMOS compatible epsilon-near-zero metamaterial for two-color ultrafast all-optical switching. *Communications Physics, 7*(1), 164.

Pradhan, J.K., Achanta, V.G., Agarwal, A.K., & Ramakrishna, S.A. (2020). Performance enhancement due to a top dielectric coating on a metamaterial perfect absorber. *Applied Optics, 59*(17), E118-E125. https://doi.org/10.1364/AO.388145.

Ren, Z., Lin, Z., Zhi, X., & Li, M. (2020). Double-layer broadband perfect metamaterial absorber and its potential for refractive index sensing. *Optical Materials, 99*, 109575. https://doi.org/10.1016/j.optmat.2019.109575.

Rensberg, J., Zhou, Y., Richter, S., Wan, C., Zhang, S., Schöppe, P., Schmidt-Grund, R., Ramanathan, S., Capasso, F., Kats, M.A., & Ronning, C. (2017). Epsilon-near-zero substrate engineering for ultrathin-film perfect absorbers. *Physical Review Applied, 8*(1), 014009.

Rhee, J., Yoo, Y., Kim, K., Kim, Y., & Lee, Y. (2014). Metamaterial-based perfect absorbers. *Journal of Electromagnetic Waves and Applications, 28*(13), 1541-1580.

Kumar, R., & Mitra, A. (2023). Inverse design of dynamically tunable phase-change material based metamaterial absorber induced structural color. *Photonics and Nanostructures-Fundamentals and Applications*, *54*, 101135. https://doi.org/10.1016/j.photonics.2023.101135.

Şanlı, A.K., Tabaru, T.E., & Kılıç, V.T. (2024). Triple band diamond-shaped polarization insensitive plasmonic nano emitter for thermal camouflage and radiative cooling. *Optical and Quantum Electronics, 56*(6), 1074. https://doi.org/10.1007/s11082-024-06970-y.

Shakiba, L., Salehi, M.R., & Emami, F. (2024). A multiband perfect metamaterial absorber based on phase change material for switching and biosensing applications. *Optics Communications, 560*, 130498. https://doi.org/10.1016/j.optcom.2024.130498.

Shrivastava, V.P., Kumar, J., & Sivakumar, S. (2017). On the controlled isotropic shrinkage induced fine-tuning of photo-luminescence in terbium ions embedded silica inverse opal films. *AIP Advances, 7*(12), 125027. https://doi.org/10.1063/1.5003692.

Shrivastava, V.P., Kumar, J., & Sivakumar, S. (2018). Enhanced green upconversion emission from α-nayf4:yb, er nanoparticles embedded silica inverse opal heterostructure. *ChemPhotoChem, 2*(8), 734-742. https://doi.org/10.1002/cptc.201800079.

Shrivastava, V.P., Radhawal, K., Rawat, S., & Khare, R. (2023). A transparent zinc oxide based metamaterial for perfect absorption of long- wavelength and mid-wavelength infrared spectral bands. *Materials Today Communications, 36*, 106714. https://doi.org/10.1016/j.mtcomm.2023.106714.

Sun, K., Riedel, C.A., Wang, Y., Urbani, A., Simeoni, M., Mengali, S., Muskens, O.L. (2018). Metasurface optical solar reflectors using AZO transparent conducting oxides for radiative cooling of spacecraft. *ACS Photonics, 5*(2), 495-501. https://doi.org/10.1021/acsphotonics.7b00991.

Wang, B.X., Qin, X., Duan, G., Yang, G., Huang, W.Q., & Huang, Z. (2024a). Dielectric-based metamaterials for near-perfect light absorption. *Advanced Functional Materials,* 2402068. https://doi.org/10.1002/adfm.202402068.

Wang, Y., Li, X., Wu, S., Hu, C., & Liu, Y. (2024b). Design of metamaterial perfect absorbers in the long-wave infrared region. *Physical Chemistry Chemical Physics, 26*(1), 551-557.

Watts, C.M., Liu, X., & Padilla, W.J. (2012). Metamaterial electromagnetic wave absorbers. *Advanced Materials, 24*(23), OP98-OP120. https://doi.org/10.1002/adma.201200674.

Wu, D., Lei, L., Xie, M., Xu, P., & Xu, S. (2023). High-performance metamaterial light absorption from visible to near-infrared assisted by anti-reflection coating. *Photonics, 10*(9), 998. https://doi.org/10.3390/photonics10090998.

Xiong, Y., Chen, F., Cheng, Y., & Luo, H. (2022). Ultra-thin optically transparent broadband microwave metamaterial absorber based on indium tin oxide. *Optical Materials, 132*, 112745. https://doi.org/10.1016/j.optmat.2022.112745.

Yu, K., Zhang, W., Qian, M., Shen, P., & Liu, Y. (2023). Multiband metamaterial emitters for infrared and laser compatible stealth with thermal management based on dissipative dielectrics. *Photonics Research, 11*(2), 290-298. https://doi.org/10.1364/PRJ.476109.

Zhang, X., Qiu, J., Li, X., Zhao, J., & Liu, L. (2020). Complex refractive indices measurements of polymers in visible and near-infrared bands. *Applied Optics, 59*(8), 2337-2344.

Publisher's Note- Ram Arti Publishers remains neutral regarding jurisdictional claims in published maps and institutional affiliations.